

# EXPERIMENTAL STUDY OF HYDROGEN RELEASE ACCIDENTS IN A VEHICLE GARAGE

Merilo, E.G.<sup>1</sup>, Groethe, M.A.<sup>2</sup>, Colton, J.D.<sup>3</sup> and Chiba, S.<sup>4</sup>

<sup>1</sup> Poulter Laboratory, SRI International, Menlo Park, CA, 94025, USA, erik.merilo@sri.com

<sup>2</sup> Poulter Laboratory, SRI International, Menlo Park, CA, 94025, USA, mark.groethe@sri.com

<sup>3</sup> Poulter Laboratory, SRI International, Menlo Park, CA, 94025, USA, james.colton@sri.com

<sup>4</sup> SRI International, 2 Ichibancho, Chiyoda-ku, Tokyo 102-0082 Japan, schiba@sri.co.jp

## ABSTRACT

Storing a hydrogen fuel cell vehicle in a garage poses a potential safety hazard because of the accidents that could arise from a hydrogen leak. A series of tests examined the risk involved with hydrogen releases and deflagrations in a structure built to simulate a one-car garage. The experiments involved igniting hydrogen gas that was released inside the structure and studying the effects of the deflagrations. The “garage” measured 2.72 m high, 3.64 m wide, and 6.10 m long internally and was constructed from steel using a reinforced design capable of withstanding a detonation. The front face of the garage was covered with a thin, transparent plastic film. Experiments were performed to investigate extended-duration (20 to 40 min.) hydrogen leaks. The effect that the presence of a vehicle in the garage has on the deflagration was also studied. The experiments examined the effectiveness of different ventilation techniques at reducing the hydrogen concentration in the enclosure. Ventilation techniques included natural upper and lower openings and mechanical ventilation systems. A system of evacuated sampling bottles was used to measure hydrogen concentration throughout the garage prior to ignition, and at various times during the release. All experiments were documented with standard and infrared (IR) video. Flame front propagation was monitored with thermocouples. Pressures within the garage were measured by four pressure transducers mounted on the inside walls of the garage. Six free-field pressure transducers were used to measure the pressures outside the garage.

## 1.0 INTRODUCTION

There are more than 65 million residential garages in the United States: 91% of all single-family homes have a garage, and 83% of these homes have a 2-car or larger garage[1]. Storing a hydrogen fuel cell car in a garage can pose a safety hazard if there is a leak from the fuel storage system that results in a buildup of a flammable mixture within the structure or within the vehicle.

Previous and ongoing research has investigated numerically and experimentally the concentration distribution for various venting scenarios in a variety of structures[2-8]. Specific recommendations have been made for venting within a single-car garage for possible leak scenarios[9], and those recommendations were used as a basis for constructing a full-scale blast-hardened structure in which hydrogen release and deflagration experiments were performed.

A series of tests was conducted to examine the risk involved with hydrogen releases and deflagrations in a structure built to simulate a one-car garage. Hydrogen releases lasting 20 to 40 min. were studied using natural ventilation or a constant mechanical ventilation rate inside the structure. The hydrogen concentration levels were measured, followed by the ignition of the flammable gas mixture. Flame speed and overpressure were measured to characterize the resulting deflagration. The natural ventilation configuration and the mechanical ventilation configuration had different upper vent openings, hydrogen release points, and spark ignition locations. Two tests were performed with a vehicle inside the garage using the natural ventilation configuration.

## 2.0 EXPERIMENTAL FACILITY

The garage facility was constructed from steel to withstand an internal detonation of a flammable gas mixture. The internal dimensions of the facility measured 2.72 m high, 3.64 m wide, and 6.10 m long.

The open end of the garage was covered with a sheet of 0.0076-mm-thick high-density polyethylene (HDPE) for the tests. Fig. 1 shows the garage facility, the HDPE cover, ventilation openings, and a reference origin. In this paper the locations (X-m , Y-m , Z-m) of ventilation ducts, sensors, sample stations, and ignition points are referenced to the origin shown in Fig. 1(a): the lower corner on the back wall of the enclosure.



Figure 1. Garage facility with mechanical (a and b) and natural (c) ventilation configurations.

For both the natural ventilation and the mechanical ventilation configurations, a ventilation opening measuring 1.22 m wide by 0.09 m high and having an area of  $0.11 \text{ m}^2$  was located near the bottom of the HDPE sheet on the open end of the facility. The center of this ventilation opening was located at  $X = 6.10 \text{ m}$ ,  $Y = 1.82 \text{ m}$ , and  $Z = 0.17 \text{ m}$ . For the natural ventilation tests a circular ventilation opening with an area of  $0.11 \text{ m}^2$  was located near the top of the HDPE sheet, centered 2.42 m above the floor (6.10 m, 1.82 m, 2.42 m). Fig. 1(c) shows the locations for the natural ventilation openings. These vents meet the size recommendations for upper and lower openings specified in the 2002 ICC Final Action Agenda[9] of  $0.046 \text{ m}^2$  open area per  $28.3 \text{ m}^3$  of garage volume ( $\frac{1}{2} \text{ ft}^2$  per  $1000 \text{ ft}^3$ ). The mass flow rate through the openings was not monitored for the natural ventilation test.

In the mechanical ventilation tests, an exhaust duct with a variable speed fan was located at the back of the garage, centered 2.42 m above the floor (0.0 m, 1.82 m, 2.42 m). Fig. 1(a) shows the location of the mechanical ventilation duct at the back of the facility. The ventilation duct was 0.34 m in diameter and 3.05 m long. A screen was placed across the front of the inlet to aid in development of the flow, and a variable-speed fan was placed at the outlet. Ventilation rates were measured using a hot wire anemometer. The flow velocity profile was measured at a point located 2.75 m from the inlet inside the duct. The flow velocity profile was measured inside the duct by placing the anemometer at seven different heights and taking the 10-s average at a given location[10]. The velocities measured at these locations were then averaged in proportion to the circular area represented by the measurement point to obtain the average bulk flow velocity. The anemometer was then placed at the centerline of the ventilation tube, documenting the flow for at least 10 min. prior to a test to obtain an average velocity that could then be used to obtain an average volumetric ventilation flow rate for the garage.

Two tests were conducted to evaluate what effect a vehicle inside the garage has on hydrogen concentrations and any resulting combustion. The vehicle used for these tests was a 1993 Ford Explorer having dimensions of 4.46 m (L), 1.78 m (W), and 1.73 m (H), similar to a potential future fuel-cell vehicle. When the Explorer was parked in the garage, its front bumper was 0.82 m from the rear wall.

Different release locations were used in the natural and mechanical ventilation configurations. In both configurations the release was directed upward toward the ceiling. In the natural ventilation configuration, the release point was located at the approximate location of the fuel cell vehicle refueling interface (4.85 m, 2.75 m, 1.00 m) for tests with and without a vehicle present. In the mechanical ventilation tests, the release point was located close to the floor in the center of the garage (3.04 m, 1.83 m, 0.25 m). The hydrogen release rate was controlled using either a Tescom 44-5200 or 44-2800 series regulator to set the pressure upstream of the nozzle. The nozzle was a Fox Valve critical flow venturi (sonic choke). For release rates  $\geq 6.7 \text{ kg/hr}$  the venturi throat diameter was 1.7 mm. For releases  $\leq 5.0 \text{ kg/hr}$  the throat diameter was 1.2 mm. Once the hydrogen passed through

the throat it entered a diffuser section designed for pressure recovery where the flow became subsonic. The hydrogen then flowed from the diffuser through a 75-mm-long by 7.75-mm inner-diameter tube, which released the hydrogen into the garage. Nozzle pressure was measured using a Lucas Schaevitz P2i53-0009 or a Sensotec TJE pressure gauge. The tank pressure was measured using a Sensotec Model TJE pressure transducer. Temperature was measured with a type T thermocouple. In the mechanical ventilation tests, the hydrogen release rate was measured by a Model 10A Thermal Mass Flowmeter made by Fox Thermal Flow Instruments. In the natural ventilation tests, an isentropic release calculation was performed using the tank pressure measurement, which was correlated with the rate measured by the mass flowmeter. The correlation was within 5% of the thermal mass flowmeter measurement over the range of release rates tested.

A system of evacuated sampling bottles was used to measure hydrogen concentration at various points throughout the garage. Each sample bottle was open for 3 s. The average fill time for a bottle was about 1 s. Samples were taken at heights of 1.9 m, 2.3 m, and 2.7 m at the center of the garage ( $X=2.8$  m,  $Y=1.8$  m), next to the center of the side wall ( $X=2.8$  m,  $Y=0.2$  m), and in a back corner ( $X=0.3$  m,  $Y=0.1$  m). These sample stations are shown in Fig. 2 (b). The sample bottle concentration was measured after each test using an H2Scan<sup>TM</sup> palladium-nickel variable-resistance hydrogen sensor.

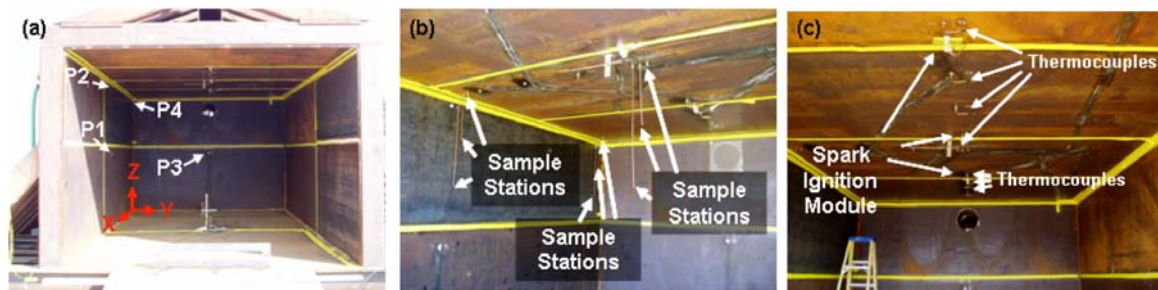


Figure 2. (a) Pressure transducer {P}, (b) sample station, and (c) thermocouple and spark ignition module locations.

Attempts were made to ignite the hydrogen and air mixture for both test configurations using multiple sparks at a variety of locations at different times. In all tests, ignition occurred during the release. The natural and mechanical ventilation tests were conducted during different testing periods, and the ignition system was altered after the natural ventilation tests. For the natural ventilation configuration, DuPont bridge wires, located on the ceiling, were used as the spark source. The bridge wires were actuated with a capacitive discharge unit (CDU) having a total energy of about 40 joules. The mixture was ignited by either the first bridge wire to spark, which was located at the center of the garage (2.72 m, 1.84 m, 2.69 m), or by the bridge wire located above the release point (4.85 m, 2.75 m, 2.69 m), which sparked 0.75 s later.

To ignite the mixture in the mechanical ventilation tests, multiple Invensys model number U-6734 electronic spark ignition modules were used. These modules were located on the ceiling of the garage and next to the release jet. When activated, the spark ignition module produces 15-millijoule sparks at a rate of a few times per second. Each module on the ceiling was individually turned on for 5 s and then turned off. Five seconds later, the next spark module was turned on for 5 s. Five seconds after the last ceiling spark module was turned off, the first spark module next to the release jet was turned on for 5 s. The dwell interval between the spark modules next to the release jet was 1 s. This approach was used to ensure that there was only a single ignition point for the mixture. Mixture ignition for all the mechanical ventilation tests occurred either at the first spark location on the ceiling (4.60 m, 1.82 m, 2.68 m) or at the spark location adjacent to the release plume (3.07 m, 1.77 m, 0.40 m).

Medtherm microsecond-responding thermocouples were used to measure the flame front time-of-arrival (TOA) and to determine the location of the ignition. The thermocouples were mounted to the ceiling of the garage and in some cases next to the release jet. Fig. 2(c) shows thermocouples mounted

on the ceiling of the garage. The thermocouples located on the ceiling were placed in groups of three to measure the flame speed propagating in different directions. The flame speeds independently determined from standard and IR video recordings are in good agreement with the thermocouple data[11].

The blast overpressure generated within the garage was measured using four pressure transducers mounted on the inside walls. Fig. 2(a) shows the pressure transducers located inside the garage. Six free-field pressure transducers were used to measure the overpressures outside the garage. All six outside transducers were mounted flush with the ground. PCB Piezotronics model 112M343 quartz pressure transducers were used for all measurements. The zero-time reference for the overpressure and impulse waveforms is the spark that ignited the gas mixture. All the overpressure data has been low-pass filtered in the frequency domain using a cutoff frequency of 1000 Hz with a cosine-shaped transition width of 200 Hz. Table 1 gives the locations of the pressure transducers inside and outside the garage.

Table 1. Pressure gauge locations.

Sensor Location	Inside				Outside			
	P1	P2	P3	P4	P5	P7	P8	P10
X (m)	2.79	2.80	0.00	0.20	11.14	16.12	6.40	6.40
Y (m)	0.00	0.00	1.82	0.00	1.82	1.82	-3.26	-8.13
Z (m)	1.37	2.62	1.38	2.62	-0.30	-0.30	-0.30	-0.30

Weather conditions were monitored during each experiment using a Davis Vantage Pro weather station. The weather data were continuously logged and stored on a computer for reference. Parameters such as air temperature, wind velocity, wind direction, barometric pressure, humidity, and rain were recorded.

### 3.0 TEST RESULTS

The garage test configuration, measured release rates, and measured ventilation rates are shown in Table 2. The concentration profiles that develop when hydrogen is released inside an enclosure are influenced by the magnitude of the release momentum and the buoyancy forces. Vertical stratified ceiling layers can form when buoyancy forces dominate[12]. Conversely when momentum forces are dominant overturning of the gas under the ceiling can occur, which can lead to the development of a well mixed ceiling layer that extends down from the ceiling into the enclosure.

The distance over which the momentum forces play a critical role in the development of a vertical release jet,  $L_m$ , has been given by Morton[13] and Hunt[14] as:

$$L_m = 0.63\alpha^{-1/2} \frac{M_o^{3/4}}{F^{1/2}} = 0.96w_o \sqrt{\frac{D_o\rho_a}{g(\rho_a - \rho_{H_2})}}, \quad (1)$$

where  $F$  is buoyancy flux,  $F = w_o g \pi ((\rho_a - \rho_{H_2}) / \rho_a) \cdot (D_o / 4)$  [15]  $M_o$  is the release momentum,  $M_o = w_o \pi D_o^2 / 4$  [15],  $\alpha$  is the plume entrainment coefficient, taken to be 0.09,  $w_o$  is the initial velocity, m/s,  $D_o$  is the nozzle diameter, m,  $g$  is the gravitational acceleration, m/s<sup>2</sup>,  $\rho_a$  is the density of air, kg/m<sup>3</sup>, and  $\rho_{H_2}$  is the density of hydrogen, kg/m<sup>3</sup>.  $L_m$  has been calculated for ambient conditions in each of the tests, given in Table 2. The calculation shows that for all tests with the exception of Test 3, where  $L_m=1.8$  m, momentum forces will be dominant when the release plume reaches the ceiling at 2.72 m. This indicates that overturning will occur near the ceiling and that a well-mixed ceiling layer is likely to be formed.

Table 2. Garage release test matrix.

Test No.	Garage Interior	H <sub>2</sub> Release Rate (kg/hr)	H <sub>2</sub> Mass Released (kg)	Calculated Exit Velocity (m/s)	L <sub>m</sub> (m)	Release Duration	Ventilation
<i>Natural Ventilation</i>							
1	Empty	9.22	3.07	668	18.7	20 min.	Natural
2	Vehicle	9.04	3.01	653	18.3	20 min.	Natural
3	Vehicle	0.88	0.44	63	1.8	30 min.	Natural
<i>Mechanical Ventilation</i>							
4	Empty	3.30	2.20	240	6.7	40 min.	0.12 m <sup>3</sup> /s
5	Empty	3.33	2.22	247	6.9	40 min.	0.19 m <sup>3</sup> /s
6	Empty	3.27	2.18	241	6.8	40 min.	0.42 m <sup>3</sup> /s
7	Empty	6.70	4.47	502	14.1	40 min.	0.10 m <sup>3</sup> /s
8	Empty	1.65	1.10	124	3.5	40 min.	0.10 m <sup>3</sup> /s
9	Empty	1.52	1.01	113	3.2	40 min.	0.20 m <sup>3</sup> /s
10	Empty	1.55	1.03	116	3.2	40 min.	0.38 m <sup>3</sup> /s
11	Empty	4.92	3.28	367	10.3	40 min.	0.10 m <sup>3</sup> /s
12	Empty	4.98	3.32	361	10.1	40 min.	0.19 m <sup>3</sup> /s
13	Empty	4.92	3.28	369	10.1	40 min.	0.38 m <sup>3</sup> /s

### 3.1 Natural Ventilation Garage Configuration Test Results

#### Hydrogen Concentration Measurements

Concentrations were sampled at three heights, three different locations, and at three separate times during a release. In this paper the concentrations that were measured at the same height and time have been averaged. Fig. 3 shows plots of the average concentration at different elevations inside the garage, sampled at three times during the release for the three tests using natural ventilation. The concentration data from the 9-kg/hr release tests (Tests 1 and 2) show the formation of a flammable ceiling layer with a relatively uniform concentration. In these releases the momentum-induced forces dominate the buoyancy forces and flow overturning occurs leading to the formation of a relatively uniform concentration ceiling layer[5]. The differences in the concentrations measured at different heights are within the scatter of the measurement technique. The concentration in the garage with a vehicle inside increased slightly more rapidly than the concentration in the empty garage. The concentration data measured in Test 3, with a release rate of 0.88 kg/hr, indicate the formation of vertically stratified concentration layers. This was the only release where the momentum forces were not dominant near the ceiling, and it was the only test in this series with signs of stratification.

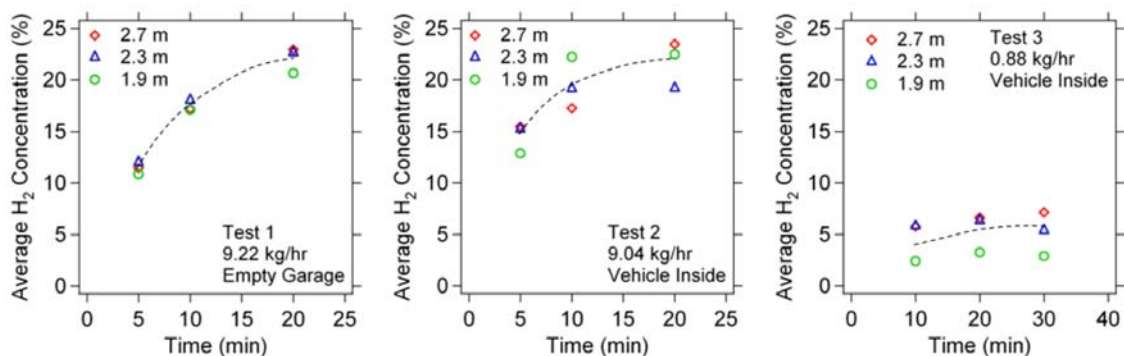


Figure 3. Average hydrogen concentration over the duration of the release for Tests 1, 2, and 3.

Table 3 gives the average hydrogen concentrations in the garage at three different heights at the time of ignition. The hydrogen concentrations at the top of the garage were similar at the time of ignition for the tests with an empty garage (Test 1) and the garage with a vehicle inside (Test 2).



Table 3. Average hydrogen concentration in the garage at time of ignition.

Test No.	Garage Interior	H <sub>2</sub> Release Rate (kg/hr)	Release Duration	Average H <sub>2</sub> Concentration at Ignition Time (%)		
				2.7 m	2.3 m	1.9 m
1	Empty	9.22	20 min.	23.0	22.6	20.7
2	Vehicle	9.04	20 min.	23.5	19.2	22.5
3	Vehicle	0.88	30 min.	7.1	5.4	2.9

*Flame Front Propagation and Flame Speed*

In Test 1 with an empty garage and Test 2 with a vehicle inside the garage, the ignition occurred at the center of the ceiling. Fig. 4 shows IR video frames, referenced to the ignition time, for Tests 1 and 2. Fig. 5 shows TOA plots and flame speed measured by fast response thermocouples on the garage ceiling, in the -X, +X and -Y directions. The highest velocity was measured in the +X direction, which was caused by the expansion of burned gas out the open end of the garage. The data show that there was a small increase in flame front velocity when the vehicle was present. This increase is probably caused by the blockage created by the presence of the vehicle inside the garage. If this is the case, it appears that the enhancement of the deflagration caused by the external surface of the vehicle is small. This result will be discussed further in the section on overpressure.

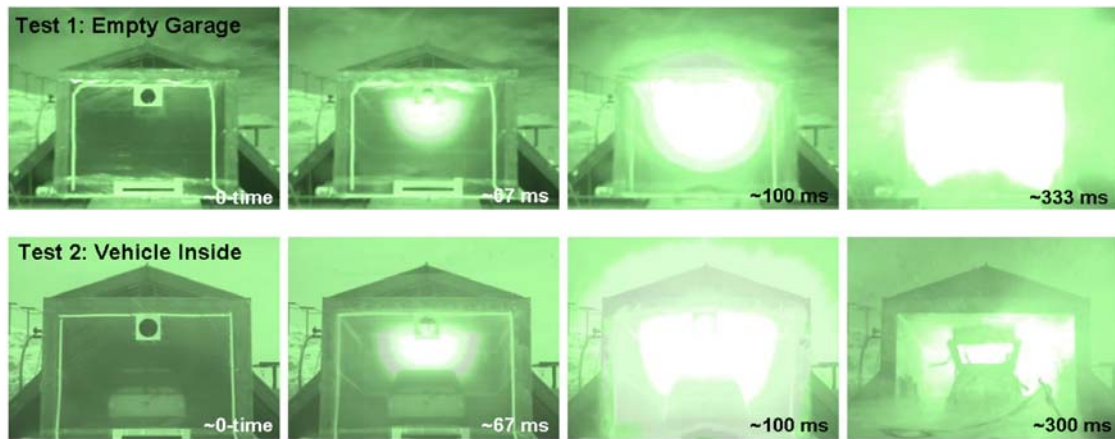


Figure 4. IR video frames from Test 1 with an empty garage and Test 2 with a vehicle inside.

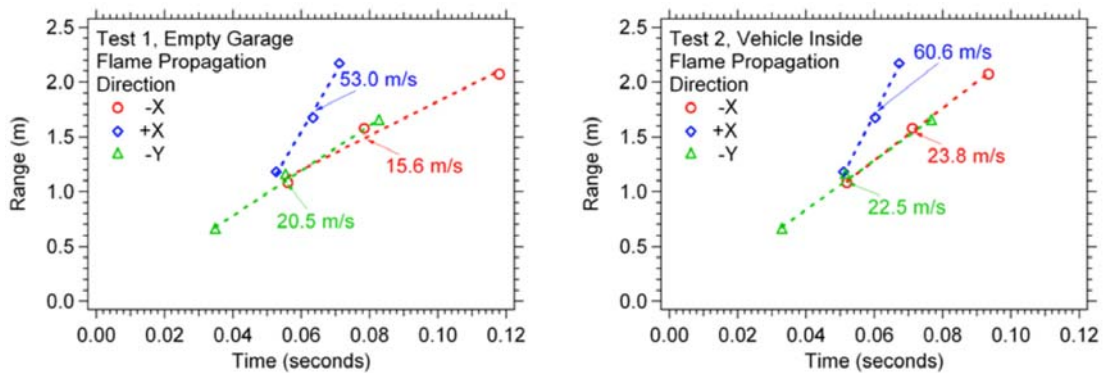


Figure 5. Flame front TOA on garage ceiling.

The flame speeds measured by the fast-response thermocouples and the IR video in each of the three natural-ventilation garage tests are given in Table 4. The results show reasonable agreement between the thermocouple and the IR data in the -Y direction. In Test 3 the ignition occurred above the release point where the hydrogen jet impinged on the ceiling. The local concentration near the impingement point was likely higher than the concentrations measured at the sample locations. The flame

propagated across the ceiling toward the back of the garage; however, no flame was visible in the IR video. After Test 3, post-test samples of the enclosure showed the presence of a hydrogen-air mixture that was below the lower flammability limit, indicating the flame was confined to a location near the ceiling.

Table 4. Measured flame speed.

Test No.	Garage Interior	H2 Release Rate (kg/hr)	Flame Speed (m/s)					
			Fast Response TC			IR Video		
			-X	+X	+Y	+Y	-Y	-Z
1	Empty	9.22	15.6	53.0	20.5	20	22	22
2	Vehicle	9.04	23.8	60.6	22.5	17	18	--
3	Vehicle	0.88	0.7	1.5	1.0	--	--	--

### Vehicle Damage

The condition of the vehicle after Test 2 clearly indicates that an internal explosion occurred within the engine compartment and inside the cabin. When the deflagration was ignited on the ceiling of the garage, the flame propagated into the interior of the vehicle. The post-test photos of the vehicle for Test 2 are shown in Fig. 6. The windows on each side of the vehicle and the rear window were shattered and the glass was thrown out from the cabin. The windshield was shattered but remained in place. The roof of the vehicle was bowed outward. The hood of the vehicle was dislodged from the engine compartment and the outer hood panel was separated from the inner hood panel. The inner hood panel flipped over and landed on top of the engine, while the outer hood panel landed next to the vehicle. The trunk of the vehicle, which was not latched for post-test safety reasons, was forced open and impacted the roof of the garage. The results show that the hydrogen-air mixture extended below the level of the hood of the car. This flammable gas mixture was able to spread into the cabin and engine compartment through air gaps in the vehicle body. The deflagration of the hydrogen-air mixture did not set the vehicle or any of its components on fire.



Figure 6. Pre-test and post-test photos of damage to the vehicle caused by an internal hydrogen-air deflagration.

### Overpressure and Impulse

Overpressure and impulse waveforms measured in Tests 1 and 2, both inside and outside the garage, are shown in Fig. 7. The plots show a significant enhancement in overpressure and impulse for the test where a vehicle was inside the garage. A sudden increase in overpressure occurred about 0.085 s after ignition in Test 2. This increase can probably be attributed to the enhancement of the deflagration as it propagates through the congested region inside the engine compartment and inside the cabin of the vehicle. Before the sudden increase in overpressure in Test 2, the pressure magnitude is only slightly higher than that generated in Test 1. This may indicate that the blockage created by the external surface of the vehicle in the garage only leads to a slight increase in overpressure and the large increase in overpressure is caused by the propagation of the deflagration inside and through the vehicle. This result has important implications for computational modeling of this type of accident scenario. It shows that to accurately predict overpressure and impulse, calculations must account for the internal geometry of the vehicle.

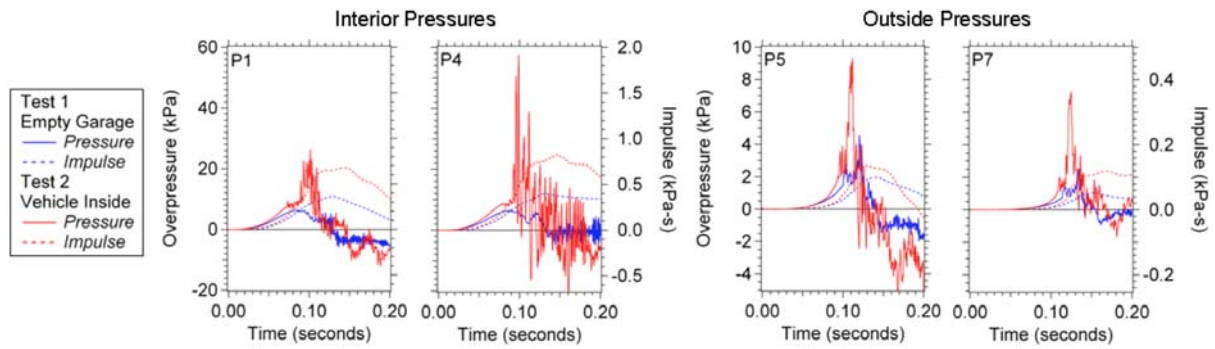


Figure 7. Overpressure and impulse waveforms from Test 1 and Test 2.

The overpressure hazard that is generated when a hydrogen release is ignited can be characterized by the peak overpressure and the peak impulse. The overpressure waveforms measured in these tests are highly structured. The frequency of the fluctuations is significantly higher than the dominant frequency of the waveform, and the peaks themselves have very low impulse values. To compare the overpressure data from each of the tests, the peak was averaged over the time span where the peak occurs and an average peak value was assigned. Determination of the peak impulse is straightforward. Table 5 gives the average peak overpressure and impulse measured in Tests 1 and 2. In Test 3 no measurable overpressure was produced. The results show that the presence of the vehicle in the garage caused the peak pressure to increase by about three times inside the garage and about two times outside the garage. The impulse was doubled both inside and outside the garage.

Table 5. Average peak overpressure and impulse.

	<b>Test 1</b>		<b>Test 2</b>	
Configuration	Empty		Vehicle	
Release Rate	9.22 kg/hr		9.04 kg/hr	
Release Duration	20 min.		20 min.	
Sensor	Pressure (kPa)	Impulse (kPa-s)	Pressure (kPa)	Impulse (kPa-s)
P1	6.3	0.36	20.5	0.68
P2	6.3	0.36	18.7	0.64
P3	7.0	0.45	23.0	0.70
P4	6.4	0.40	30.6	0.83
P5	4.6	0.10	8.4	0.14
P7	2.6	0.05	6.9	0.12
P8	4.6	0.08	7.2	0.10
P10	1.6	0.04	3.2	0.05

### 3.2 Mechanical Ventilation Garage Configuration Test Results

#### *Hydrogen and Natural Gas Concentration Measurements*

Concentrations taken at the center of the garage, near the side wall, and in a back corner were averaged for a given height and time. Fig. 8(a) shows plots of these average concentrations for three different elevations inside the garage over the duration of the release for Test 7. This plot shows that the concentration in the garage had reached a relatively steady state by the time samples were taken at 26 min. after the start of the release. Table 6 gives the average hydrogen concentrations in the garage taken at three heights just prior to ignition. The differences in the concentrations measured at different heights are within the scatter of the measurement technique. The concentration in the upper portion of the garage appeared to be well mixed for all the mechanical ventilation tests. This indicates that the momentum of the release caused the formation of a well-mixed layer. The mechanical ventilation may also have played a role. This result was typical for all tests performed using mechanical ventilation.



The concentrations measured at all nine sample locations in the garage at the end of the 40-min. release have been averaged for the purpose of comparison. These values represent the average concentration in the buoyant ceiling layer of the garage. Fig. 8(b) shows a plot of the average hydrogen concentrations in the upper portion of the garage plotted against the hydrogen release rate and ventilation rate. This plot shows that the mechanical ventilation was effective at reducing the hydrogen concentrations in the garage.

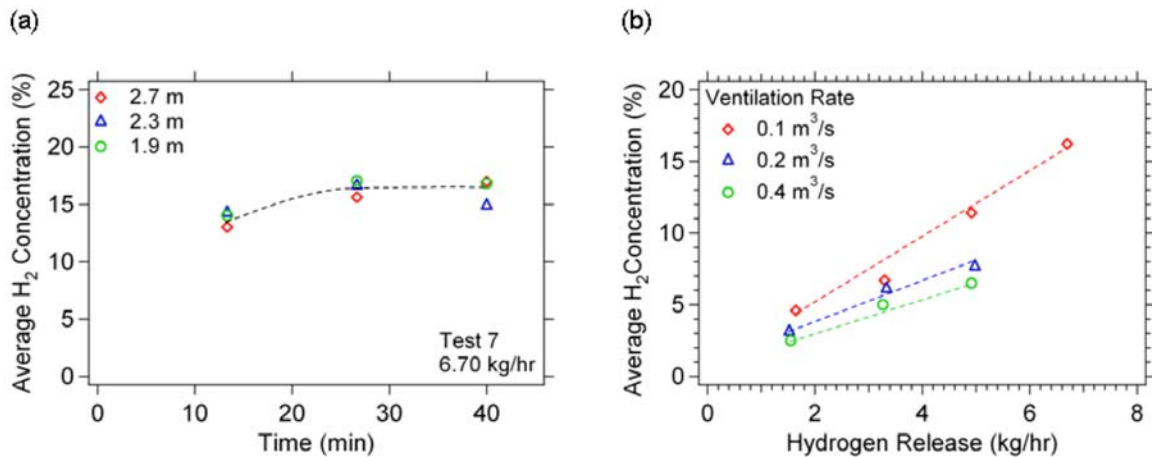


Figure 8. (a) Average hydrogen concentration over the duration of the release for Test 7. (b) Average concentration in the upper portion of the garage at time of ignition.

Table 6. Concentration from garage tests with mechanical ventilation.

Test No.	Release Rate (kg/hr)	Ventilation (m <sup>3</sup> /s)	Average Gas Concentration at Ignition Time (%)		
			2.7 m	2.3 m	1.9 m
4	3.30	0.12	6.7	6.1	7.2
5	3.33	0.19	6.6	5.0	6.8
6	3.27	0.42	5.2	4.7	5.0
7	6.70	0.10	17.0	14.9	16.8
8	1.65	0.10	4.9	4.3	4.7
9	1.52	0.20	3.5	3.0	2.6
10	1.55	0.38	2.5	2.5	2.4
11	4.92	0.10	12.3	10.4	11.6
12	4.98	0.19	8.1	7.2	7.6
13	4.92	0.38	7.2	5.4	6.8

### Flame Front Propagation and Flame Speed

In the mechanical ventilation tests, the first attempt to ignite the hydrogen-air mixture was made on the ceiling near the open end of the facility (4.60 m, 1.82 m, 2.68 m). If the mixture could not be ignited on the ceiling, a spark located near the release plume (3.07 m, 1.77 m, 0.40 m) ignited the release and a jet fire was formed. When ignition occurred on the ceiling, the fast-response thermocouples could be used to measure the flame speed as the flame front propagated toward the back of the garage. Fig. 9(a) shows IR video frames from the Test 7 deflagration. Fig. 9(b) is a TOA plot with flame speed measured by the fast-response thermocouples in the -X direction. This test produced the highest flame speed of all the tests performed in this series. The TOA plot shows that the flame front accelerated slightly as it propagated toward the back of the garage. The slight acceleration of the flame front occurred for all seven tests that were ignited at the ceiling. Table 7 lists the flame speed measured by the fast-response thermocouples from 0.36 to 1.56 m and from 2.82 to 3.81 m referenced to the ignition location.

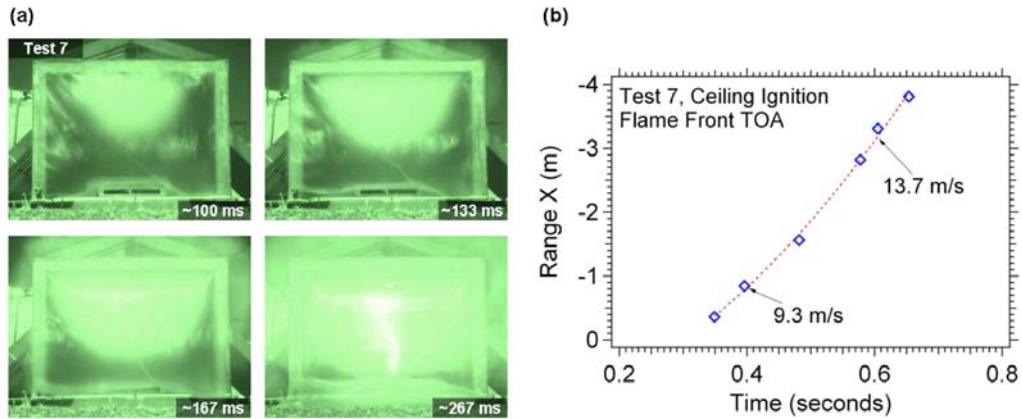


Figure 9. Flame speed data from Test 7 with a 6.70 kg/hr release and 0.1 m<sup>3</sup>/s ventilation rate. (a) IR video frames, (b) Thermocouple TOA data.

Table 7. Flame speed from thermocouple measurements in garage tests with mechanical ventilation.

Test No.	Release Rate (kg/hr)	Ventilation (m <sup>3</sup> /s)	Flame Speed -X (m/s)	
			0.36 - 1.56 m	2.82 - 3.81 m
4	3.30	0.12	0.5	1.3
5	3.33	0.19	0.6	2.2
6	3.27	0.42	0.4	1.7
7	6.70	0.10	9.3	13.7
11	4.92	0.10	3.2	6.2
12	4.98	0.19	1.2	2.0
13	4.92	0.38	1.0	2.3

### Overpressure and Impulse

Of the eleven tests performed in the garage with mechanical ventilation, only Test 7, with a release rate of 6.70 kg/hr and a ventilation rate of 0.10 m<sup>3</sup>/s, produced overpressures significant enough to constitute a hazard. Fig. 10 shows the pressure and impulse waveforms measured in Test 7. Table 8 gives the average peak overpressure and impulse measured in garage tests with mechanical ventilation. The overpressure generated in Test 7 was well below a level that would cause eardrum rupture[16]; however, it could potentially launch projectiles. The overpressure generated in Test 7 was about 10 times greater than the pressures generated by other tests in this series.

The tests performed with a release rate of 4.9 kg/hr produced very small overpressures in the garage when the mixture was ignited at the ceiling. Overpressures were not detected for tests with hydrogen release rates of 1.6 kg/hr and 3.3 kg/hr when the gas mixture was ignited near the ceiling of the garage. Small overpressures were observed for these release rates when the hydrogen jet was ignited. This is due to the turbulence of the jet and the higher concentrations of hydrogen at the ignition location. When the release jet was ignited, the overpressures produced in the garage were usually about 0.04 kPa. For release rates  $\leq 4.9$  kg/hr, the primary hazard is the deflagration and the hydrogen jet fire inside the garage.

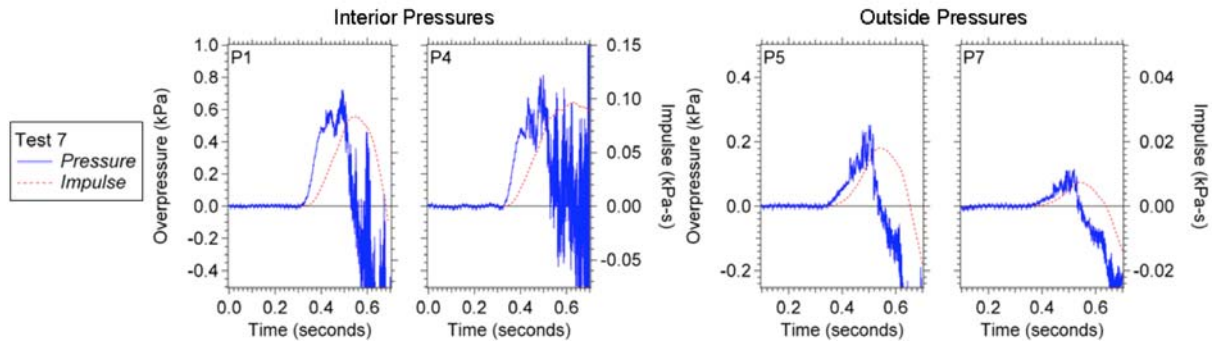


Figure 10. Overpressure and impulse waveforms from Test 7.

Table 8. Average peak overpressure and impulse measured inside the garage.

Test No.	P1		P2		P3		P4	
	Pressure	Impulse	Pressure	Impulse	Pressure	Impulse	Pressure	Impulse
	(kPa)	(Pa-sec)	(kPa)	(Pa-sec)	(kPa)	(Pa-sec)	(kPa)	(Pa-sec)
4	0.04	1.46	--	--	0.04	0.85	--	--
5	0.03	0.65	--	--	0.04	0.54	--	--
6	0.07	1.23	0.05	0.67	0.11	1.22	0.12	1.07
7	0.64	83.8	0.58	79.7	0.77	114.0	0.74	97.3
8	0.04	0.64	0.05	0.65	0.07	0.66	0.08	0.72
9	0.04	0.56	0.06	1.81	0.05	0.56	0.06	1.59
10	0.04	0.37	--	--	0.07	0.79	--	--
11	0.05	11.40	0.03	4.95	0.05	16.54	0.04	14.24
12	0.02	0.17	0.02	0.34	0.03	1.34	0.04	4.69
13	0.03	18.85	--	--	0.04	41.27	--	--

#### 4.0 SUMMARY AND CONCLUSIONS

Three tests were performed in a blast-hardened garage facility using natural ventilation. Two of the tests were performed with a release rate of 9 kg/hr at the refueling interface of a fuel cell vehicle, one test with an empty garage and one with a vehicle inside the garage. The concentrations measured in the upper portion of the garage in both of these tests were relatively well mixed and similar at the time of ignition. Fast-response thermocouple measurements showed only a slight increase in flame speed on the roof of the garage when a vehicle was present. However, the extensive damage to the vehicle showed that an internal explosion occurred within the engine compartment and inside the cabin. This result indicates that the buoyant ceiling layer extended below the hood of the car and that a flammable gas mixture was able to collect inside the vehicle and under the hood. When the deflagration was ignited at the ceiling, the flame front propagated into the vehicle cabin and engine compartment, where turbulent enhancement led to the significant increase in the observed overpressure. The measurements for the test with a vehicle show a sudden increase in overpressure at about 0.085 s after ignition, which is about the expected time for the flame front to reach the vehicle from the ignition location. Average peak overpressures were tripled inside the garage and doubled outside the garage. The result shows that the internal geometry of the vehicle needs to be taken into account when computationally modeling this type of accident scenario. One natural ventilation test was performed with a release rate of 0.88 kg/hr with a vehicle inside the garage. Concentrations measured in this test were very lean. A flame was detected propagating across the top of the garage; however, no overpressure was detected.

Ten tests were performed in the garage using mechanical ventilation. Tests were performed with hydrogen release rates of 1.6 kg/hr, 3.3 kg/hr, 4.9 kg/hr, and 6.7 kg/hr and ventilation rates of 0.1 m<sup>3</sup>/s, 0.2 m<sup>3</sup>/s, and 0.4 m<sup>3</sup>/s. All the release scenarios resulted in well-mixed lean mixtures below the ceiling. Increased ventilation rates showed a reduction in hydrogen concentration for all the tests. The

maximum concentration and overpressure obtained in the mechanical ventilation test configuration were produced with a 6.7-kg/hr release and a ventilation rate of 0.1 m<sup>3</sup>/s (Test 7). In this test the average hydrogen concentration in the upper portion of the garage was 16.2% and the maximum average peak overpressure was 0.769 kPa. For the release rates ≤4.9 kg/hr, the primary hazard was the deflagration of the hydrogen and air mixture and the burning of the hydrogen jet fire inside the garage. For all the mechanical ventilation tests except the 6.70 kg/hr release, the overpressures that resulted from the confined deflagrations were all very low and did not represent a risk to people or property.

## ACKNOWLEDGMENTS

These studies were performed for the Institute of Applied Energy (IAE) and administered through the New Energy and Industrial Technology Development Organization (NEDO) as part of the “Establishment of Codes & Standards for Hydrogen Economy Society” program, with funding from the Agency of National Resources and Energy (ANRE) in the Ministry of Economy, Trade and Industry (METI) of Japan.

## REFERENCES

1. National Association of Home Builders Housing Facts, Figures, and Trends, 2004.
2. Swain, M.R., Shriber, J. and Swain, M.N., Comparison of Hydrogen, Natural Gas, Liquefied Petroleum Gas, and Gasoline Leakage in a Residential Garage, *Energy Fuels*, **12**, No. 1, 1998, pp. 83-89.
3. Swain, M.R., Filoso, P., Grilliot, E.S., and Swain, M.N, Hydrogen Leakage into Simple Geometric Enclosures, *Int. J. of Hydrogen Energy*, **28**, 2003, pp. 229-248.
4. Bédard-Tremblay, L., Fang, L., Bauwens, L., Finstad, P.H.E, Cheng, Z. and Tchouvelev, A.V., Simulation of Detonation After and Accidental Hydrogen Release in Enclosed Environments, Proceedings of the 2<sup>nd</sup> ICHS Conference, 11-13 September 2007, San Sebastian, Spain.
5. Hunt, G.R. and Linden, P.F., Steady-state Flows in an Enclosure Ventilated by Buoyancy Forces Assisted by Wind. *Journal of Fluid Mechanics*, **426**, 2001, pp. 355-386.
6. Lacombe, J.M., Dagba, Y., Perrette, L., Jamois, D. and Proust, C.H., Large Scale Hydrogen Release in an Isothermal Confined Area, Proceedings of the 2<sup>nd</sup> ICHS Conference, 11-13 September 2007, San Sebastian, Spain.
7. Gupta, S., Brinster, J., Studer, E. and Tkatschenko, I., Hydrogen Related Risks Within a Private Garage: Concentration Measurements in a Realistic Full Scale Experimental Facility, Proceedings of the 2<sup>nd</sup> ICHS Conference, 11-13 September 2007, San Sebastian, Spain.
8. Barley, C.D., Gawlik, K., Ohi, J. and Hewett, R., Analysis of Buoyancy-Driven Ventilation of Hydrogen from Buildings, Proceedings of the 2<sup>nd</sup> ICHS Conference, 11-13 September 2007, San Sebastian, Spain.
9. 2002 ICC Final Action Agenda, M7-02, 304.3, Section 1307.4, p. 461, [www.iccsafe.org/cs/codes/2002cycle/faa02imc.PDF](http://www.iccsafe.org/cs/codes/2002cycle/faa02imc.PDF)
10. Ishimoto, Y., Merilo, E.G., Groethe, M.A., Chiba, S., Iwabuchi, H. and Sakata, K., Study of Hydrogen Diffusion and Deflagration in a Closed System, Proceedings of the 2<sup>nd</sup> ICHS Conference, 11-13 September 2007, San Sebastian, Spain.
11. Merilo, E.G. and Groethe, M.A., Deflagration Safety Study of Mixtures of Hydrogen and Natural Gas in a Semi-Open Space, Proceedings of the 2<sup>nd</sup> ICHS Conference, 11-13 September 2007, San Sebastian, Spain.
12. Baines, W.D. and Turner, J.S., Turbulent buoyant convection from a source in confined region, *Journal of Fluid Mechanics*, **37**, 1969, pp. 51-80.
13. Morton, B.R. Forced plumes, *Journal of Fluid Mechanics*, **5**, 1959, pp. 151-163.
14. Hunt, G.R. and Kaye, N.G., Virtual origin correction for lazy turbulent plumes, *Journal of Fluid Mechanics*, **435**, 2001, pp. 377-396.
15. Turner J.S. Buoyant plumes and thermals, *Annual Reviews of Fluid Mechanics*, **1**, 1969, pp.29-44.
16. Hirsch, F.G., Effects of Overpressure on The Ear – Review, *Annals of the New York Academy of Sciences*, **152**, No. 1, pp. 147-162.